Supporting Information

The Hydrolysis Mechanism of the Anticancer Ruthenium Drugs NAMI-A and ICR Investigated by DFT-PCM Calculations.

Attilio V. Vargiu,[a,b,c,±] Arturo Robertazzi,[a,b,c,±] Alessandra Magistrato,[b,a,c,*] Paolo Ruggerone[d,b] and Paolo Carloni[a,b,c]

[a]SISSA (ISAS), Via Beirut 4, I-34014 Trieste (Italy); [b]CNR-INFM Democritos National Simulation Center; [c]Italian Institute of Technology (IIT); Via Beirut 2-4, Trieste, I-34014; [d]CNR-INFM SLACS and Dipartimento di Fisica, Università di Cagliari, S.P. Monserrato-Sestu Km 0.700, I-09042 Monserrato (Italy).

[±] equally contributed to this work

[*] corresponding author

Comparison between calculated and experimental structures.

Agreement between DFT optimised and experimental NAMI-A structures is fairly good, as discussed in Computational Details and displayed in Tab. 1 and Tab. S1. However, in order to further test the accuracy of DFT calculations, properties of NAMI-A^{II} were calculated at the MP2 level as displayed in Tab. S2. Geometries of NAMI-A optimised at B3LYP/6-31G(d,p) only slightly differ from that obtained at MP2/6-31G(d,p). Indeed, the largest difference of coordination bond lengths (Ru-Cl, Ru-S, Ru-N and Ru-O) is 0.06 Å. Also angles and dihedral angles were well described by B3LYP (data not shown). In addition, formation energy of PI_{Cl} from NAMI-AII in vacuo were estimated at DFT-B3LYP and MP2 level. Calculated values differ by less than 3 kcal/mol, indicating the reliability of DFT-B3LYP calculations for this study.

Partial dissociative and associative (I_D and I_A) mechanisms have been proposed to be the most significant in ligand-water exchange reactions for octahedral complexes.[1-3] To investigate the relevance of such mechanisms, test calculations on the first hydrolysis step of NAMI-A were performed following both I_D and I_A, Figure S1. As expected,[1-3] the I_D mechanism turns out to be more favorable than I_A. Indeed, almost all the hydrolysis paths studied proceed *via* I_D.

Tab. S1. Geometrical parameters of NAMI-A calculated with larger basis sets and with/without the inclusion of the solvation model during optimization

	Expt. [4]	6-31G(d,p) [GAS]	6-31G(d,p)[PCM]	6-311+G(d,p) [GAS]	6-311+G(d,p)[PCM]
Ru-Cl	2.34	2.43	2.43	2.44	2.43
Ru-S	2.30	2.40	2.44	2.41	2.44
Ru-N	2.08	2.10	2.10	2.10	2.10

Tab. S2. DFT *vs*. MP2 coordination bond lengths of NAMI-A^{II}

	B3LYP/6-31G(d,p)	MP2/6-31G(d,p)
Ru—Cl1	2.60	2.54
Ru—Cl2	2.55	2.50
Ru—Cl3	2.50	2.47
Ru—Cl4	2.56	2.51
Ru—S	2.32	2.30
Ru—N	2.10	2.06

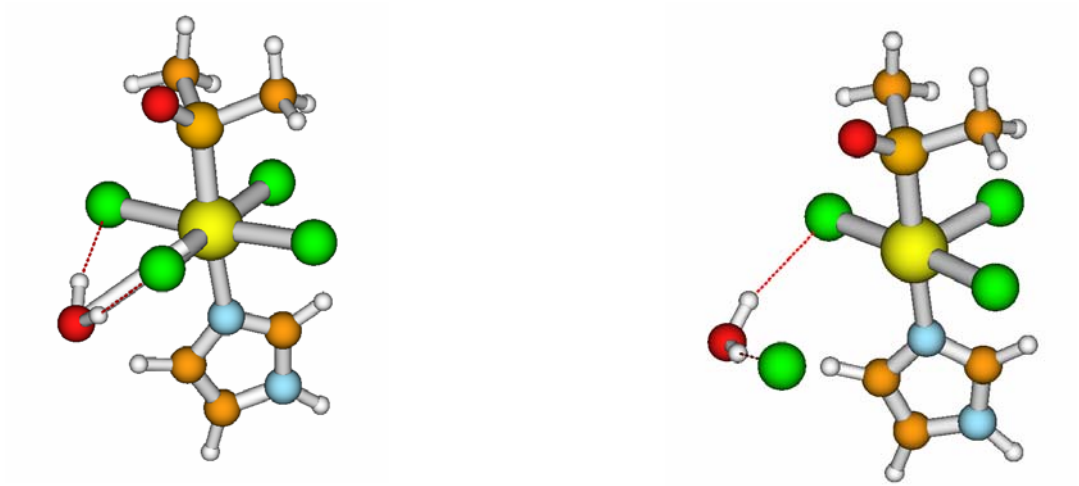

Fig. S1. Associative-Dissociative mechanism of NAMI-A^{II} at the first hydrolysis step.

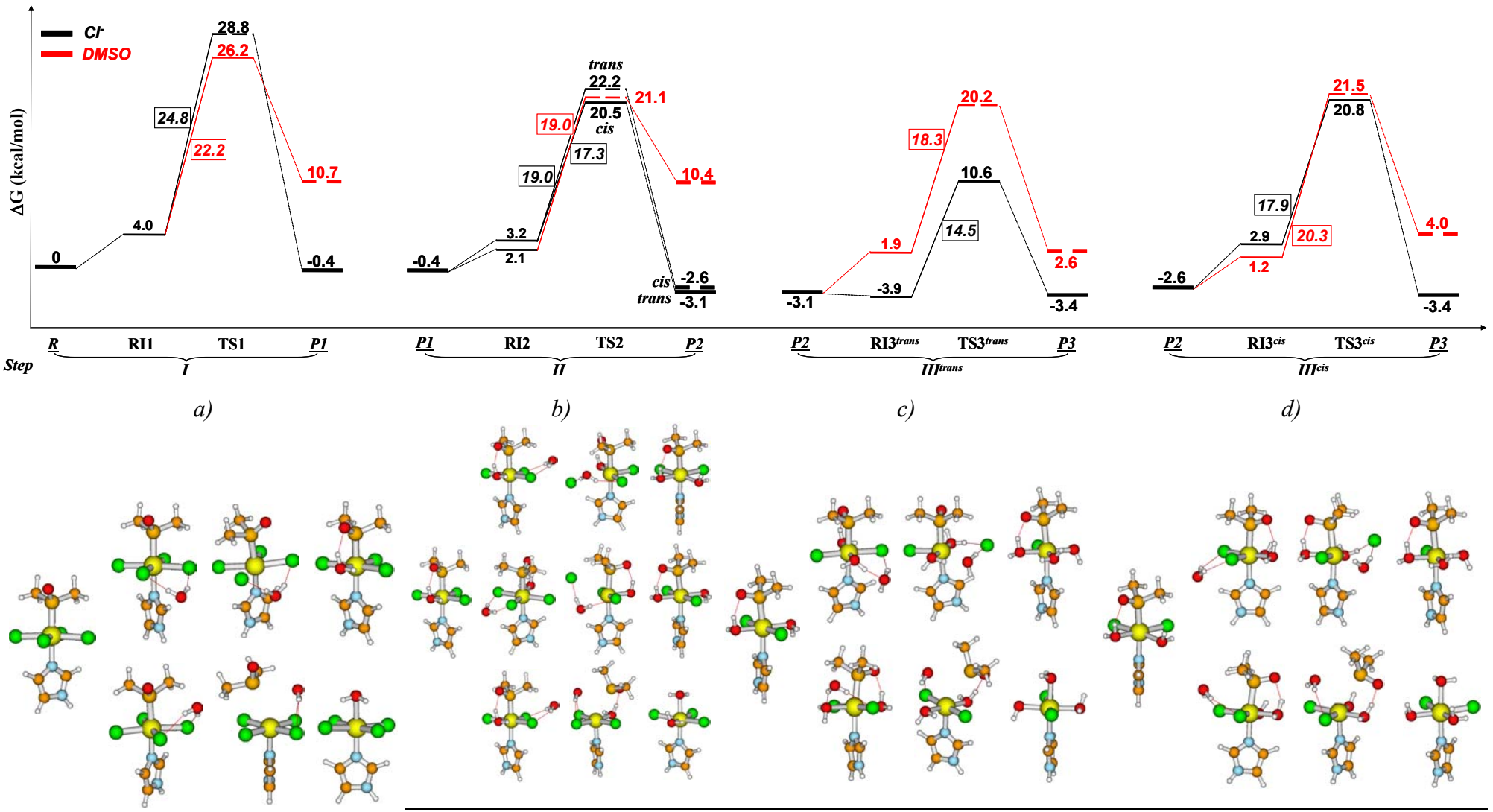

Fig. S2a. Free energy profiles of Cl^- and DMSO hydrolyses in NAMI-A^{II}: *a)* first hydrolysis; *b)* second hydrolysis; *c)* third hydrolysis starting from PII_{2Cl}^{trans} ; d) third hydrolysis starting from PII_{2Cl}^{cis} . Black and red lines correspond to Cl^- and DMSO dissociations, respectively, and metabolites without DMSO are indicated by a red line. The most favorable transition states and products are represented by solid lines, while dotted lines are used for the less likely intermediates and TS structures. Activation free energies (kcal/mol) are displayed in the squares along the reaction path. Energies reported on the lines are referred to R.

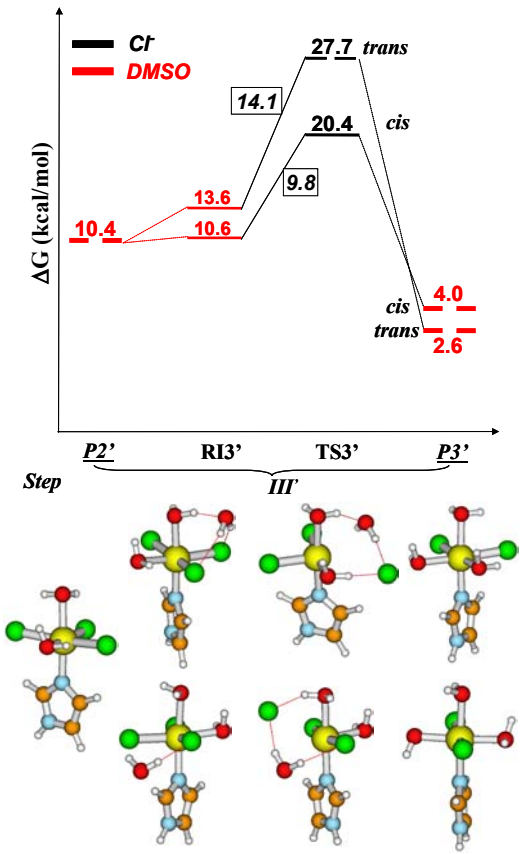

Fig. S2b. Free energy profiles for the third Cl^- hydrolysis starting from PII_{2Cl}^{trans} in NAMI-A^{II}. For further details see Fig. S2a.

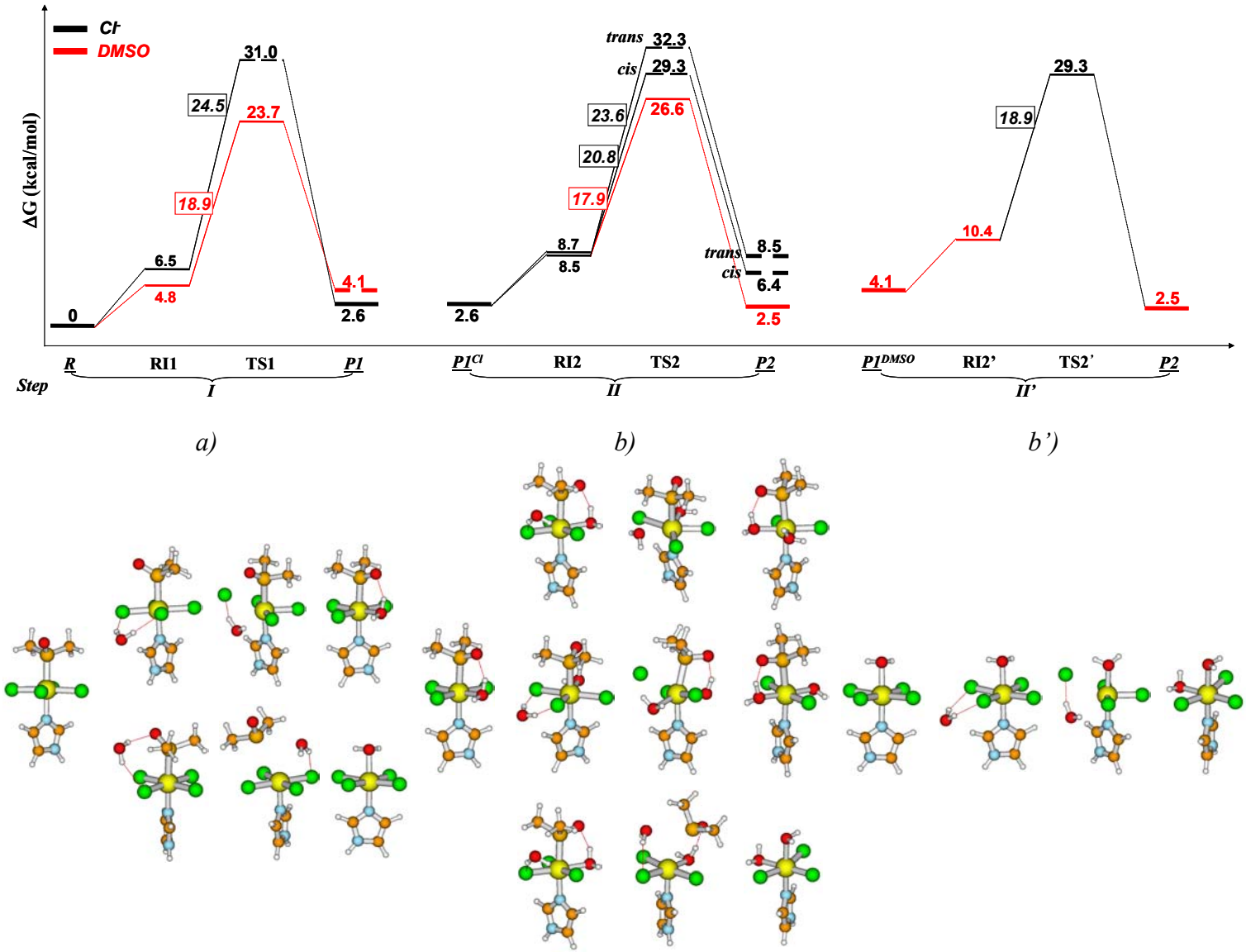

Fig. S3a. Free energy profiles of Cl^- and DMSO hydrolyses in NAMI-A^{III}: *a)* first hydrolysis; *b)* second hydrolysis from PI_{Cl}; *b')* second hydrolysis from PI_{DMSO}. For further details see Fig. S2a.

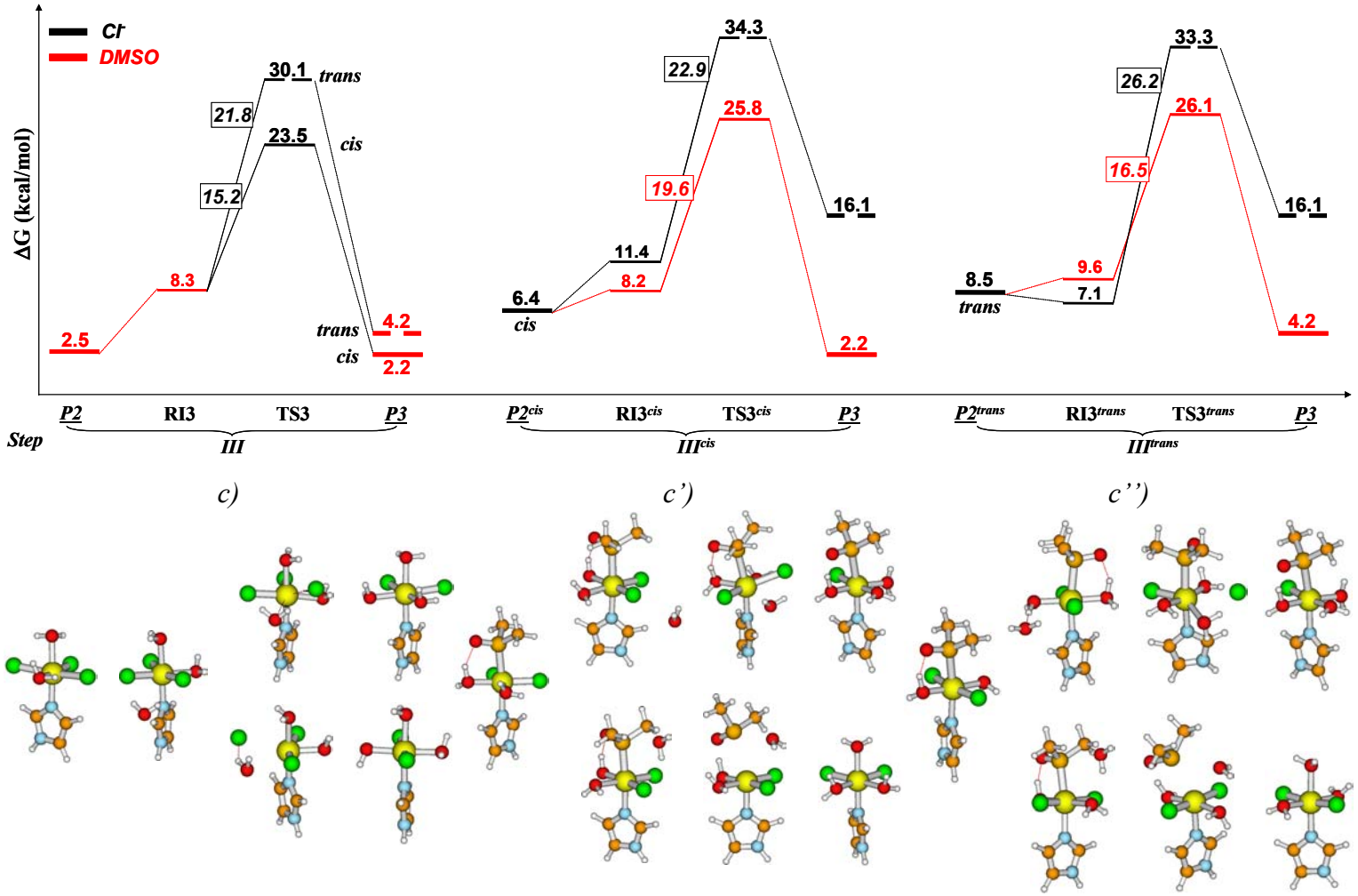

Fig. S3b. Free energy profiles of Cl^- and DMSO hydrolyses in NAMI-A^{III}: c*)* third hydrolysis from $PII_{Cl,DMSO}$; third hydrolysis from PII_{2Cl}^{cis}; third hydrolysis from PII_{2Cl}^{trans}. For further details see Fig. S2a.

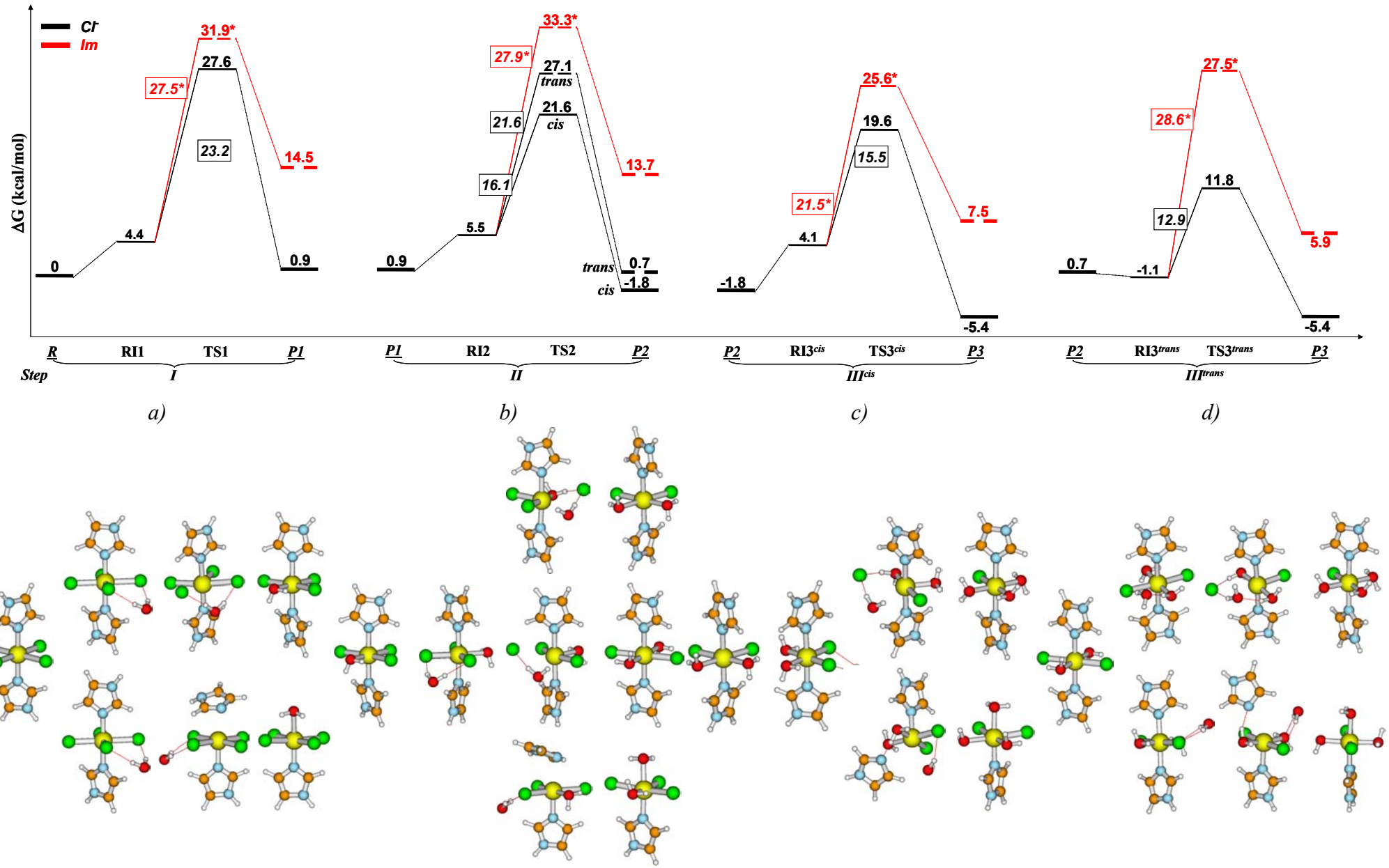

Fig. S4. Free energy profiles of Cl^- and Im hydrolyses in ICR^{II}: *a)* first hydrolysis; *b)* second hydrolysis; *c)* third hydrolysis starting from PII^{trans}_{2Cl} ; d) third hydrolysis starting from PII^{cis}_{2Cl} . For further details see Fig. S2a. * Im pseudo transition states: see Computational Details.

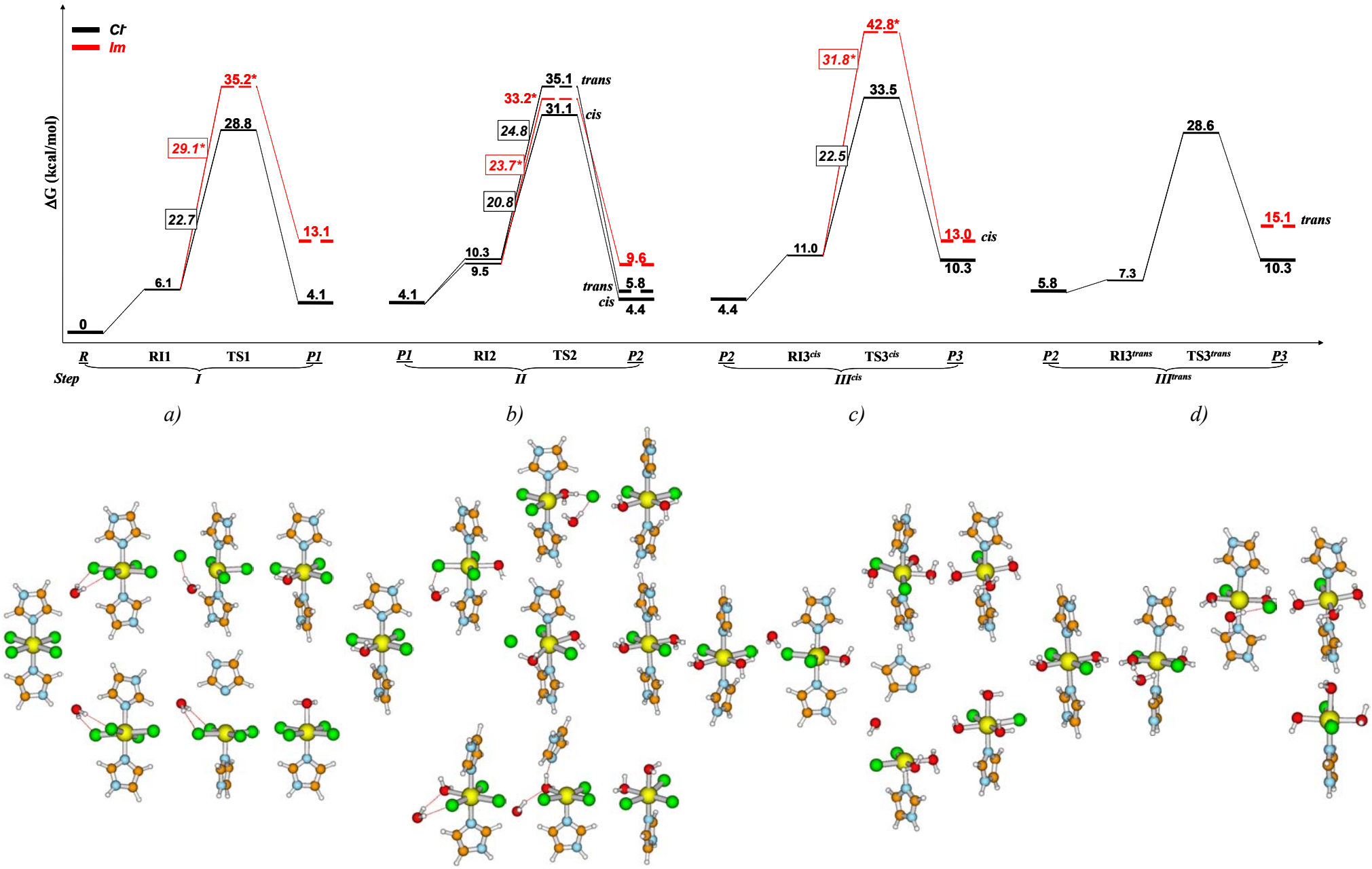

Fig. S5. Free energy profiles of Cl^- and Im hydrolyses in ICR^{III}: *a)* first hydrolysis; *b)* second hydrolysis; *c)* third hydrolysis starting from PII_{2Cl}^{trans} ; d) third

hydrolysis starting from PII_{2Cl}^{cis}. For further details see Fig. S2a. * Im pseudo transition states: see Computational Details.

REFERENCES

(1) Richens, D. T. *Chem. Rev.* 2005, *105*, 1961-2002.
(2) Swaddle, T. W. *Comm. Inorg. Chem.* 1991, *12*, 237.
(3) Lay, P. A. *Comm. Inorg. Chem.* 1991, *9*, 235.
(4) Alessio, E.; Balducci, G.; Lutman, A.; Mestroni, G.; Calligaris, M.; Attia, W. M. *Inorg. Chim. Acta* 1993, *203*, 205-217.